AD-A071 788 ELECTROCHEMICAL TECHNOLOGY CORP SEATTLE WASH F/G 11/6
EXPERIMENTAL OBSERVATIONS AND ANALYSIS OF HYDRODYNAMIC EFFECTS --ETC(U)
JUN 79 T R BECK, S G CHAN N00014-76-C-0495

UNCLASSIFIED NL

| OF |
AD A071788

END
DATE FILMED
8-79
DDC

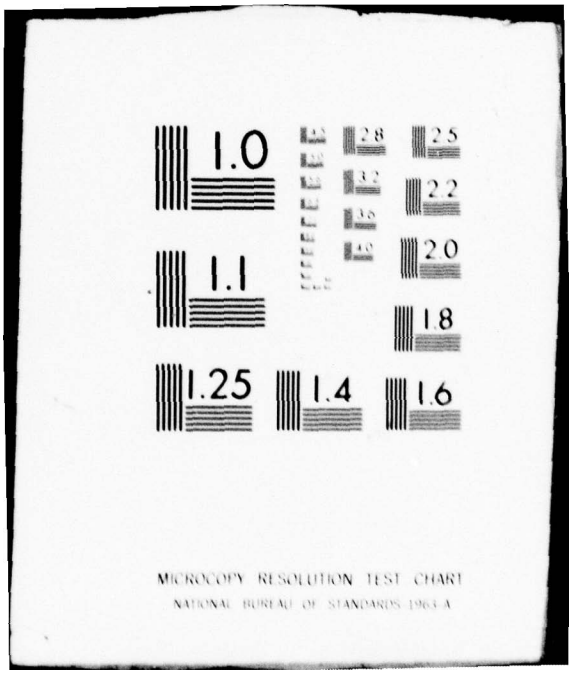
1.0
1.1
1.25
1.4
1.6
2.8
3.2
3.6
4.0
2.5
2.2
2.0
1.8
MICROCOPY RESOLUTION TEST CHART
NATIONAL BUREAU OF STANDARDS 1963-A

LEVEL

Contract N00014-76-C-0495

EXPERIMENTAL OBSERVATIONS AND ANALYSIS OF HYDRODYNAMIC EFFECTS ON GROWTH OF SMALL PITS

Manuscript

THEODORE R. BECK

ELECTROCHEMICAL TECHNOLOGY CORP.
3935 LEARY WAY N.W.
SEATTLE, WA 98107
(206) 632-5965

INTERIM REPORT FOR PERIOD MARCH 1978 - FEBRUARY 1979

Prepared for

OFFICE OF NAVAL RESEARCH
800 North Quincy Street
Arlington, VA 22217

June 1979

Unclassified

SECURITY CLASSIFICATION OF THIS PAGE (When Date Entered)

REPORT DOCUMENTATION PAGE	READ INSTRUCTIONS BEFORE COMPLETING FORM
1. REPORT NUMBER (6)	2. GOVT ACCESSION NO. (9) Interim
4. TITLE (and Subtitle): Experimental Observations and Analysis of Hydrodynamic Effects on Growth of Small Pits	5. TYPE OF REPORT & PERIOD COVERED: Technical Report, March 1978 — February 1979
	6. PERFORMING ORG. REPORT NUMBER
7. AUTHOR(s) (10) Theodore R. Beck, Sandra G. Chan	8. CONTRACT OR GRANT NUMBER(s) (15) N00014-76-C-0495
9. PERFORMING ORGANIZATION NAME AND ADDRESS: Electrochemical Technology Corp., 3935 Leary Way N.W., Seattle, WA 98107	10. PROGRAM ELEMENT, PROJECT, TASK AREA & WORK UNIT NUMBERS
11. CONTROLLING OFFICE NAME AND ADDRESS: Office of Naval Research, Materials Division, Arlington, VA 2217 (11)	12. REPORT DATE: June 1979 13. NUMBER OF PAGES: 34
14. MONITORING AGENCY NAME & ADDRESS (if different from Controlling Office) (12) 37p.	15. SECURITY CLASS. (of this report) 15a. DECLASSIFICATION/DOWNGRADING SCHEDULE

16. DISTRIBUTION STATEMENT (of this Report)

This document has been approved for public release and sale; its distribution is unlimited.

17. DISTRIBUTION STATEMENT (of the abstract entered in Block 20, if different from Report)

Reproduction in whole or part is permitted for any purpose of the United States Government. Distribution is unlimited.

18. SUPPLEMENTARY NOTES

Manuscript to be submitted to the Journal of the Electrochemical Society. This paper will be presented to the Electrochemical Society, Los Angeles, CA, October 14-19, 1979.

19. KEY WORDS (Continue on reverse side if necessary and identify by block number)

Iron, stainless steel, mass transport, salt film, ohmic resistance, corrosion.

20. ABSTRACT (Continue on reverse side if necessary and identify by block number)

Potentiostated pitting experiments were conducted with zone-refined iron and with commercial 304 stainless steel in sodium chloride solutions. Growth of single small pits initiated at small holes in a lacquer surface layer were observed under a microscope at 60X under stagnant and controlled hydrodynamic flow conditions. Three modes limiting pit growth rate were observed: hemispherical diffusion, hydrodynamic boundary layer diffusion, and solution ohmic resistance. Experiments showed that for a given size pit there is a

DD FORM 1 JAN 73 1473

392075

Unclassified

SECURITY CLASSIFICATION OF THIS PAGE (When Date Entered)

threshold velocity below which hydrodynamic flow is not important and that there is a critical velocity above which current density is limited by ohmic drop in solution. Stainless steel repassivates at the ohmic limited current density and pitting stops.

EXPERIMENTAL OBSERVATIONS AND ANALYSIS OF HYDRODYNAMIC EFFECTS ON GROWTH OF SMALL PITS

Theodore R. Beck* and Sandra G. Chan

Electrochemical Technology Corp.
3935 Leary Way N.W., Seattle, Washington 98107

ABSTRACT

Potentiostated pitting experiments were conducted with zone-refined iron and with commercial 304 stainless steel in sodium chloride solutions. Growth of single small pits initiated at small holes in a lacquer surface layer were observed under a microscope at 60X under stagnant and controlled hydrodynamic flow conditions. Three modes limiting pit growth rate were observed: hemispherical diffusion, hydrodynamic boundary layer diffusion, and solution ohmic resistance. Experiments showed that for a given size pit there is a threshold velocity below which hydrodynamic flow is not important and that there is a critical velocity above which current density is limited by ohmic drop in solution. Stainless steel repassivates at the ohmic limited current density and pitting stops.

Key words: Iron, stainless steel, mass transport, salt film, ohmic resistance, corrosion.

*Electrochemical Society Active Member

This manuscript
to be submitted to the
Journal of the Electrochemical Society

A considerable body of empirical information has been developed on the effect of seawater velocity on corrosion rate of various metals. The general corrosion rate of steel is shown to increase with velocity and become asymptotic to 35 mils per year at velocities above 20 ft/s (1). Copper-nickel alloys also corrode at a higher rate at higher water velocities (2, 3). Stainless steels, on the other hand, show less pitting attack at increased velocity and a velocity greater than 5 ft/s is recommended to avoid pitting in seawater (1, 2).

Increased general corrosion with velocity can be related to increased transport of oxygen to the surface to provide a cathodic current to drive the corrosion reaction; this has been qualitatively discussed for copper-nickel alloys (3). The purpose of the present work is to develop a quantitative framework for relating decreased pitting of stainless steels with flow velocity.

In recent years it has become generally recognized that solution conditions inside of pits in various metals are different from bulk conditions outside. Saturated metal salt solutions may form (4), salt films may precipitate (5-10), the solution may become acid by hydrolysis of the metal salt (11), the potential is more active than outside (9, 12), and hydrogen gas may be generated (9, 12). Models have been presented for the mass transport of various ionic and molecular species in stagnant pits (10-12). Experimental observations have also been presented for the effect of solution velocity in a channel on pitting current in an artificial one-dimensional pit in the channel wall for titanium and for iron (13). The present work extends the hydrodynamic experiments to smaller, more-realistic pits in iron and stainless steel.

Experimental

A cell was designed, Fig. 1, in which a metal under study is mounted flush to the wall of a flow channel. A glass window forms the opposite wall of the channel so that pits on the metal surface can be observed under a microscope. The channel has a 0.25 cm x 0.32 cm, cross section. The working electrode is a rectangular rod, polished flat and square on the end with No. 600 silicon carbide paper. The working electrodes are 0.16 cm x 0.32 cm in cross section and are mounted to fill the 0.32 cm channel width. A similar silver rod is mounted upstream to form an Ag/AgCl reference electrode and a square, 0.32 cm x 0.32 cm, platinum foil counter electrode is mounted on the channel wall downstream. The working electrodes were sealed into the cell with paraffin wax to avoid a built in crevice.

All experiments were carried out under potentiostatic conditions. A pump constructed of Teflon was used for electrolyte circulation and flow was measured with rotameters calibrated in the solutions used.

Two metals were used for the working electrodes, zone-refined iron* (14) and commercial 304 stainless steel. A typical analysis of the zone-refined iron has been published (14); in the specimen used the total nonmetallic = 4 ppm and total metallic = 27 ppm, giving 99.997% Fe by difference. An analysis of the stainless steel is given in Table 1.

---

*Provided by courtesy of the American Iron and Steel Institute.

Sodium chloride solutions and NaCl-HCl and NaCl-Na_2SO_4 solutions were made from ACS reagent grade chemicals and distilled water.

In the first experiments multiple small pits were obtained on the ends of the working electrode. The pits in the center of the specimen were all of approximately the same size and were sufficiently separated, but at the edges of the specimen where the current density tended to be higher the pits grew together into general corrosion patches. The presence of corrosion patches made it impossible to obtain accurate data on the effect of flow on a given pit size. Furthermore, transient effects due to step change in flow rate were masked by averaging large numbers of pits distributed over the surface. A single small pit was desirable.

Several methods were tried to obtain a single pit, including changing solution composition, decreasing the potential, making surface flaws with a needle point, and using various coatings with a small hole in them. The last technique was the most successful. A lacquer (fingernail polish) was applied to the surface and when dry a sewing needle tip was used to make a hole in the lacquer. A sewing needle was observed at high magnification to have a blunt tip which could be used to squeeze out a bare area the diameter of the blunt end. The displaced lacquer formed a slight crater rim. Other methods such as making holes in electronic-type photo resist coatings or in electroplaters stop-off tape were not as successful.

Results and Discussion

Initial experiments were conducted with pure iron specimens in Na_2SO_4, NaCl solutions as used by Vetter and Strehblow (5). Two solutions were

used: 0.1 N Na_2SO_4, 0.01 N NaCl, and 1 N Na_2SO_4, 0.1 N NaCl. For both electrolytes a multiplicity of pits nucleated over the surface and the pit walls were polished. The effect of electrolyte flow past the pitting surface was to increase the anodic current to the specimen as shown in Fig. 2. It was generally observed that the ratio of current with flow to that with no flow increased with time (larger pits). The final diameter of the larger pits in the center of the specimen in this experiment was 35 μm. Increase in pitting current with electrolyte velocity past the pits is clearly in accord with mass transport limited current density (13).

Further experiments were conducted with pure iron in NaCl solutions. At a concentration of 0.1 N NaCl, discrete pits were obtained but at 1 N NaCl general corrosion occurred at an early stage and pits could not be studied. At NaCl concentrations of 0.1 N and less the current to the pits decreased as flow of electrolyte was turned on. At concentrations slightly above 0.1 N the current increased with flow of electrolyte. These phenomena will be discussed later.

Pitting experiments were conducted with the 304 stainless steel in 1 N NaCl solutions over a range in pH from 1 to 6 and a range of potentials from 0.2 V to 0.8 V versus Ag/AgCl. In all cases a multitude of small pits nucleated and grew on the surface. The effect of electrolyte flow velocity in all cases was to cause an immediate decrease in current as illustrated for a typical experiment in Fig. 3. Apparently removal of corrosion products from the pits resulted in repassivation. The current increased with time while the flow was on and continued to increase when the flow was subsequently turned off. Each successive time the flow was turned on the current decreased

but not to as low a value. Visual observation under the microscope indicated crevice corrosion occurred at the edge of the specimen. Crevice corrosion would be expected to be less affected by flow than would the pits which have a smaller depth to diameter ratio.

An informative experiment was to allow the pits to grow under stagnant flow conditions until they merged into corrosion on the whole surface, and then determine the effect of flow. Results of such an experiment are given in Fig. 4. A logarithmic time scale was used in order to compress the later, slower events onto one graph. At the start of the experiment the whole 0.16 cm x 0.32 cm stainless steel surface was corroding. The surface at 1 in Fig. 4 was covered with a green salt solution and earlier analyses (10, 13) show that a salt layer was present. At the moment the electrolyte flow started the current increased, passed through a maximum and decreased. During this period the green salt layer and solution were observed to be removed. At 2 in Fig. 4 the metal surface was observed to be slightly recessed, very flat and polished. In about a second a multitude of tiny, barely visible at 60X, pits could be seen at 3 in Fig. 4. The current increased as these pits grew and went through a second maximum. At 4 in Fig. 4 the pits covered about 50% of the surface and at 5 the whole surface was corroding. At 6 the current had returned to the same condition as the starting point 1.

In this case electrolyte flow caused the current to increase initially as is expected for a mass transport limited process, but as the salt layer was removed the surface repassivated. Crevice corrosion at the edges of the specimen, however, prevented the current from going to zero. In Fig. 3

the initial decrease in current with electrolyte flow is due to averaging events that are not simultaneous over a number of small pits. Clearly, to obtain valid flow transient effects for small pits they should be studied individually.

Restrained Single Pits

A single pit artificially restrained to occur through a small hole in an insulating lacquer is illustrated in Fig. 5. The needle used to make the hole caused a slight crater rim of lacquer around the pit and a slight indentation in the metal. Most of the work was carried out with approximately-0.0035 cm radius pits; the radii of the holes in the lacquer were measured at the ends of the experiments. As pitting progressed the pit undercut the lacquer and the experiments were stopped when the radius in the plane of the metal surface was 1.5 to 2 times the radius of the hole in the lacquer. The final pits were shallower than hemispheres, with depth to surface radius ratio of about 0.5. The bottoms of the pits were generally polished with the iron and the stainless steel used.

The turn-on transient current and the effect of a pulse of electrolyte flow on current to a pit propagating in pure iron are shown in Fig. 6. The iron is immediately active when the step potential is applied and the initial peak current to the disk is determined by ohmic overpotential (15, 16).

$$i_{\Omega} = \frac{4\kappa\eta_o}{\pi r} \qquad (1)$$

The current then decays due to salt film passivation as has been reported for larger shielded electrodes (17). Subsequent pulses of electrolyte flow cause the current again to increase to the ohmic limit. The current should

be smaller than for the first peak because the pit is now deeper, but the hole in the lacquer enlarged slightly giving a larger current. The new current density peaks may be described by (5).

$$i_\Omega = \frac{\kappa\eta_o}{ar} \tag{2}$$

in which $\kappa\eta_o/r$ is the current density on a convex hemisphere limited by electrolyte resistance from a counter electrode at infinity and a is a factor to correct for the electrolyte resistance from the convex hemisphere to the concave pit surface. The factor, a, has been estimated (5) to be about 3.

After salt film passivation is established the limiting current density is approximated by (5)

$$i_L = \frac{zFDC_s}{ar} (f_t) \tag{3}$$

The effects of increased transport due to electrolytic migration (f_t factor) and decreased transport due to extra diffusion resistance from the convex hemisphere to the concave pit surface (a factor) largely cancel. Using the values z = 2, D = 0.85 x 10^{-5} cm^2/s (18), C_s = 4.1 x 10^{-3} mol/cm^3 (18), and r = 0.0035 cm gives i_L = 1.9 A/cm^2 as compared to 1.8 to 2.1 A/cm^2 determined from the plateaus in Fig. 6.

A polarization curve for the artificial pits with radius of 0.0035 cm in pure iron in 1 N NaCl at pH 1 is given in Fig. 7. Peak current densities for pulse electrolyte flow are plotted as a function of potential. An iR-corrected Tafel line is plotted using equation 2, and a conductivity of 0.125 ohm^{-1} cm^{-1} (21, 22). A best fit Tafel line was obtained with a = 2. The Tafel line is consistent with literature data (19, 20) at lower current

densities. The limiting current density for salt diffusion out of the pits is also plotted in Fig. 7. Within experimental error it is independent of potential and of electrolyte concentration from 0.01 N to 1 N NaCl.

With iron in low electrolyte concentrations the ohmic limit for bulk solution (equation 2) was less than the mass transport limited current density (equation 3), yet pitting occured at the latter value. The reason is that iron is active in chloride solutions and ferrous chloride reaction product builds up in solution in the pit, increasing electrolyte conductivity in a zone in and near the pit where it is most effective. The effect of a pulse of electrolyte flow on pit corrosion current density in a 0.01 N NaCl solution is shown in Fig. 8. The pulse was applied when the pit was in the mass-transport-limited mode and the current immediately dropped to the ohmic-limited mode. With subsequent zero electrolyte flow the current increased with $FeCl_2$ concentration until salt precipitation occured. In accordance with Sand's equation, the product of $I\tau^{1/2}$ during the recovery period until salt precipitation was approximately constant (e.g., ~ 0.4 $mA\,s^{-1}$ in Figs. 6 and 8).

It is appropriate now to consider more quantitatively the effect of electrolyte flow velocity on the limiting mass transport current density. No theory or data were found in the literature to predict limiting current density to a small circular area on the wall of a channel or pipe, although there are some related cases. Limiting current density to a rectangular electrode filling a square channel width has been measured (13). Theory and measurements have been presented for limiting current density to a small disk electrode imbedded in a larger insulating rotating disk at a

radius, R, from the center (23), and for a similar small disk electrode in an impinging jet (24). The most nearly analogous theoretical development to the present disk in the wall of a flow channel was that of Levich (25) for the limiting current density for an area in the form of a strip of width, h, and distance, ℓ, from the leading edge of a plate in a laminar flow stream. Modified for the present circumstance, this equation is,

$$i_{LC} = \frac{0.5\, zFDC_s \left(\frac{\nu}{D}\right)^{1/3} U^{1/2} (f_t)}{\nu^{1/2} h^{1/3} \ell^{1/6} a} \qquad (4)$$

The diameter of the disk (2r) may be substituted for h in equation 4. The form of the equation for the imbedded small disk electrode in an insulating rotating disk (23) is the same as equation 4 except the constant is about 0.73 instead of 0.5 and $R^{-1/6}$ replaces $\ell^{-1/6}$.

Plots of limiting current density from equation 4 versus disk radius with velocity as a parameter are given in Fig. 9. It was assumed as a first approximation that the terms, f_t, and a, cancel. Equations 2 and 3 are also plotted in Fig. 9. The parameter values used for all three equations in Fig. 9 are given in Table 2. The entrance length in a channel to the point at which the hydrodynamic boundary layers intersect was used for ℓ in equation 4. Beyond this length the flow conditions become essentially uniform. Schlichting (26) gives for the entrance length,

$$\ell_E = 0.04\, WRe \qquad (5)$$

For velocities of 8 to 266 cm/sec in a channel of width 0.32 cm, Re varies from 240 to 8400*, giving ℓ_E = 3.1 to 109 cm. (Although the straight section of channel ahead of the pit was only 2.54 cm in length, it was preceded by

*Although these data actually extend into the turbulent flow regime, equation 4 will still be used because no other relation is available.

two 90^{o} bends which caused a flow disturbance equivalent to a much longer section.) The corresponding values of $\ell^{-1/6}$ are 0.82 to 0.46; because the shape of the $\ell^{-1/6}$ versus velocity curve is relatively flat in the range of 50 to 300 cm/sec, a value of $\ell^{-1/6} = 0.5$ was used in equation 4.

Consider a pit of radius 0.0035 cm as used in most of the experiments and shown as the vertical line in Fig. 9. The pitting current density should be independent of electrolyte flow as given by equation 3 until the velocity reaches about 4 cm/s and then the limiting current density should increase according to equation 4 if $i_{\Omega} > i_{L}$. The current density should increase with velocity until $i_{LC} = i_{\Omega}$ and then remain constant at i for iron which does not repassivate. For example, 1 N NaCl and $\eta_{o} = 0.5$ V requires a velocity of about 50 cm/s to reach the ohmic limit. If $i_{\Omega} < i_{L}$ the current density should decrease with velocities greater than 4 cm/s until i_{Ω} is reached, but an equation is not available to predict the relation of i_{LC} to velocity in this case.

Fig. 9 shows that the smaller the pit the higher is the threshold velocity at which pit current density is affected. A given velocity above the threshold should also have a greater effect on current density for larger pits; this was experimentally observed as shown in Fig. 2.

The threshold velocity for electrolyte velocity to affect pitting current density can be determined by equating i_{L} of equation 3 to i_{LC} of equation 4 which gives,

$$U_{T} = 6.35\ \nu\ell^{1/3}\left(\frac{\nu}{D}\right)^{-2/3} r^{-4/3} \qquad (6)$$

The constants from Table 2 inserted in equation 6 give,

$$U_T = 2.54 \times 10^{-3} r^{-4/3} \tag{7}$$

The conductivity at which current density should be the same with and without flow may be obtained by equating i_L of equation 3 to i_Ω of equation 2 which gives,

$$\kappa = \frac{zFDC_s f_t}{\eta_o} \tag{8}$$

The breakeven conductivity using the constants in Table 2 is 0.027 $\Omega^{-1}cm^{-1}$ which corresponds to ≈ 0.27 N NaCl.

Experiments were conducted to test the effect of velocity on current density for iron in 1 N, 0.5 N and 0.02 N NaCl solutions as shown in Fig. 10. A large number of experiments was required because of considerable data scatter. The experiments confirmed that for the two higher concentrations of NaCl the current density increased with flow rate and for the 0.02 N solution the current density decreased as predicted by Fig. 9. The experimental current densities for 1 N and 0.5 N NaCl were, however, a factor of 1.3 to 2 below the prediction of equation 4. One explanation is that the convection causes a smaller concentration of $FeCl_2$ in the vicinity of the pit and thus the transference number factor approaches unity but the geometric factor, a, remains the same. At velocities above 100 cm/s the current densities are seen to asymptotically approach the ohmic limit as expected for all three solutions.

The effect of velocity on single artificial pits was also determined for stainless steel as shown in Fig. 11. The data tended to be quite non-reproducible but general trends were determined. The non-reproducibility

is largely due to two factors; gel-like hydroxide formed in the pits and was non-reproducibly removed with flow, and crevice corrosion occured in a ring surrounding the pit between the lacquer and the metal. In contrast to pure iron, the current density increased slowly with time when the potential was applied due to slow initiation of corrosion and did not reach the ohmic limit.

Even in a relatively small pit, the behavior was similar to that in Fig. 4 for the larger shielded electrode. The current density for the single pit increased with flow velocity at low velocities as expected. At the highest velocities, the current density immediately peaked at a value below the ohmic limit and then dropped to a low value. Removal of the hydroxy-chloride film allowed the metal surface to repassivate. Even at a bulk pH of 1 the surface repassivated, indicating that for 304 stainless steel the salt film is more important for maintaining pitting than low pH.

At the highest velocities the current after the rapid drop always increased with time because of increased crevice corrosion activity. Behavior was then erratic when flow was stopped due to some combined effect of decreased crevice corrosion current and reinitiation of pitting current.

Observations on stainless steel and equations 2 - 4 lead to interesting insights regarding the mechanism of prevention of pitting by electrolyte flow. Suppose that in 1 N NaCl for natural small pits the $FeCl_2$ salt layer is completely removed when the solution velocity causes i_{LC} to equal i_{Ω}. Assume also that crevice corrosion does not occur between the passive oxide film and the metal as was observed between the lacquer and the metal. Thus there is a critical velocity for each pit radius above which pitting is

suppressed, determined by the intersection if i_{LC} and i_{Ω} in Fig. 9. This critical velocity is plotted in Fig. 12 as a function of pit radius. In the region to the left of the line pitting is allowed but pitting is not allowed on the right side. If pits are able to initiate they are thus able to grow to a certain critical size depending on flow velocity and then they are suppressed.

Estimation of the critical size of pits in stainless steel at the recommended 5 ft/s velocity in seawater is of interest. The critical velocity versus pit size relationship is generalized in order to make this estimate. Based on the experimental data in Fig. 10 it will be assumed that at the critical velocity the transference number factor, f_t, is unity but the geometric factor, a, must be used in equation 4. Thus by equating i_{LC} of equation 4 to i of equation 2 and solving for the critical velocity, U_c, one obtains,

$$U_c = \frac{2.52\ \kappa^2 \eta_o^2 \nu \ell^{1/3}}{z^2 F^2 D^2 C_s^2 \left(\frac{\nu}{D}\right)^{2/3}} r^{-4/3} \qquad (9)$$

Using the values of ν, $\ell^{1/6}$, z, D, and C_s from Table 2, equation 9 reduces to,

$$U_c = 22.3\ \kappa^2 \eta_o^2 r^{-4/3} \qquad (10)$$

Equation 10 may be applied to seawater by inserting appropriate values of κ and η_o. Seawater conductivity is ~0.07 $ohm^{-1}cm^{-1}$ (27). The potential of passive 304 stainless steel in seawater is ~0.2 V_{SHE}* (28). This

---

*Stainless steels are shown to have potentials slightly active to silver.

potential gives $\eta_o \approx 0.2$ V in Fig. 7. These values of κ and η_o inserted in equation 10 give,

$$U_c = 0.0044\ r^{-4/3} \tag{11}$$

which is also plotted in Fig. 12. At a velocity of 5 ft/s (152 cm/s) the critical pit radius is seen to be about 2 μm. Thus pits can only grow to microscopic size before they are extinguished at the recommended 5 ft/s velocity. Although this conclusion applies strictly to experiments in the Fig. 1 flow cell, the relative insensitivity to position of a pit from the leading edge of a body in a flow stream ($U_c \propto \ell^{1/3}$) in equation 9 gives more general applicability in terms of order of magnitude of the maximum pit size.

Conclusions

1. Current density in pits in pure iron and in 304 stainless steel is mass transport controlled in accord with hemispherical diffusion from a salt film and saturated solution at the walls of the pit.

2. There is a threshold electrolyte velocity, past the pit mouth, varying inversely with pit radius, above which convection effects determine current density.

3. At velocities greater than the threshold, current density increases to ohmic resistance limited value in high-conductivity solution and decreases to an ohmic limit in low-conductivity solution.

4. Pits in 304 stainless steel tend to repassivate at the ohmic limit at a critical velocity where the salt film is removed.

5. The predicted critical repassivation velocity varies as pit radius to the negative 4/3 power.

6. Experimental results and analysis indicate that the maximum pit radius is a few micrometers for 304 stainless steel at the recommended minimum seawater velocity of 5 ft/s.

Acknowledgment

This investigation was supported by Office of Naval Research Contract No. N00014-76-C-0495.

Nomenclature

a = a geometric constant

C = concentration, mole/cm^3

D = diffusion coefficient, cm^2/s

f = correction factor

F = the Faraday, 96,500 C/mole

h = width of band on plate in flow stream, cm

ℓ = distance from leading edge of plate, cm

r = radius, cm

R = distance of conducting disk from center of rotation, cm

Re = Reynolds number, dimensionless

U = fluid velocity, cm/s

w = width of channel, cm

z = equiv/mole

Greek:

η = overvoltage, V

κ = conductivity $ohm^{-1}cm^{-1}$

ν = kinematic viscosity, cm^2/s

Subscripts:

C = critical velocity for repassivation

E = entrance length

L = transport limited

LC = transport limited in convection mode

o = ohmic

s = saturation

t = transference

T = threshold velocity for convection effect

Ω = ohmic limited

References

1. F. L. LaQue, "Behavior of Metals and Alloys in Seawater," p 383, in Corrosion Handbook, H. H. Uhlig, Ed., John Wiley, New York (1948).

2. F. L. LaQue, Marine Corrosion, p 138, John Wiley, New York (1975).

3. B. C. Syrett, Corrosion, 32, 242 (1976).

4. H. Kaesche, Z. Physik, Chem., (N.F.), 34, 87 (1962).

5. K. J. Vetter and H. H. Strehblow, Localized Corrosion, R. W. Staehle, et al. Eds., December 1971, p 240, NACE, Houston, 1974 and Ber. Bunsenges. Physik. Chem. 74, 1024 (1970).

6. H. J. Engell, Electrochim. Acta, 22, 987 (1977).

7. Yu. A. Popov and Ya. M. Kolotyrkin, Zhur. Fiz. Khim. 51, 3121 (1979); Ya. A. Popov, Y. V. Alekseev, Ya. M. Kolotyrkin, and A. A. Vasil'ev, ibid, 51, 2726 (1977).

8. I. L. Rosenfeld, I. S. Danilov, and R. N. Oranskaya, This Journal, 125, 1729 (1978).

9. T. R. Beck, This Journal, 120 1317 (1973).

10. T. R. Beck and R. C. Alkire, Accepted by J. Electrochem. Soc., 1979.

11. J. R. Galvele, This Journal, 123, 464 (1976).

12. H. W. Pickering and R. P. Frankenthal, This Journal, 119, 1297 (1972).

13. T. R. Beck, Corrosion, 33, 9 (1977).

14. C. W. Marschall, J. D. Myers, and G. W. P. Rengstorff, Metals Engineering Quarterly, February, 1974.

15. H. S. Carslaw and J. C. Jaeger, Conduction of Heat in Solids, p 214, 2nd ed., Oxford University Press, 1959.

16. J. Newman, This Journal, 113, 501 (1966).

17. T. R. Beck, Submitted to J. Electrochem. Soc.

18. H. C. Kuo and D. Landolt, Electrochim. Acta, 20, 393 (1975).

19. E. J. Kelly, This Journal, 112, 124 (1965).

20. H. C. Kuo and K. Nobe, This Journal, 125, 853 (1978).

21. R. A. Robinson and R. H. Stokes, Electrolyte Solutions, p 466, 2nd ed., Butterworths, London, 1959.

22. B. E. Conway, Electrochemical Data, p 141, Elsevier, New York, 1952.

23. D-T. Chin and M. Litt, This Journal, 119, 1338 (1972).

24. D-T. Chin and C-H. Tsang, This Journal, 125, 1461 (1978).

25. V. G. Levich, Physicochemical Hydrodynamics, (Engl. Translation), p 344, Prentice Hall, Englewood Cliffs, N.J., 1962.

26. H. Schlichting, Boundary Layer Theory, (Engl. Translation), p 149, Pergamon, New York, 1955.

27. R. W. Weast, Ed., CRC Handbook of Chemistry and Physics, 58th ed., D-249, CRC Press, Cleveland, Ohio, 1977.

28. M. G. Fontana and N. D. Greene, Corrosion Engineering, p 32, McGraw Hill, New York, 1967.

Table 1

Composition of 304 stainless steel used in experiments (chemical analysis).

Component	Percent
Ni	8.38
Cr	18.74
C	0.07
Mn	1.94
P	0.019
S	0.012
Si	0.53
Mo	0.36
Cn	0.26

Table 2

Parameter values used in equations 2, 3, and 4, plotted in Fig. 9.

κ for NaCl solutions (21)

C (N)	κ ($\Omega^{-1}cm^{-1}$)
0.01	0.00118
0.02	0.00232
0.05	0.00555
0.1	0.0107
0.2	0.203
0.5	0.0468
1.0	0.858

$\eta_o = 0.5V$

$a = 2$ (Eq. 2) $\quad f_t/a = 1$ (Eq. 3)

$z = 2$

$D = 0.85 \times 10^{-5}$ cm^2/sec (18)

$C_s = 4.1 \times 10^{-3}$ mol/cm^3 (18)

$\nu = 0.01$ cm^2/sec

$\ell^{-1/6} \approx 0.5$ (see text)

$\therefore$ Eq. 2 $\quad i_\Omega = 0.25\, \kappa r^{-1}$

Eq. 3 $\quad i_L = 6.73 \times 10^{-3} r^{-1}$

Eq. 4 $\quad i_{LC} = 0.133\, U^{1/2} r^{-1/3}$

List of Figures

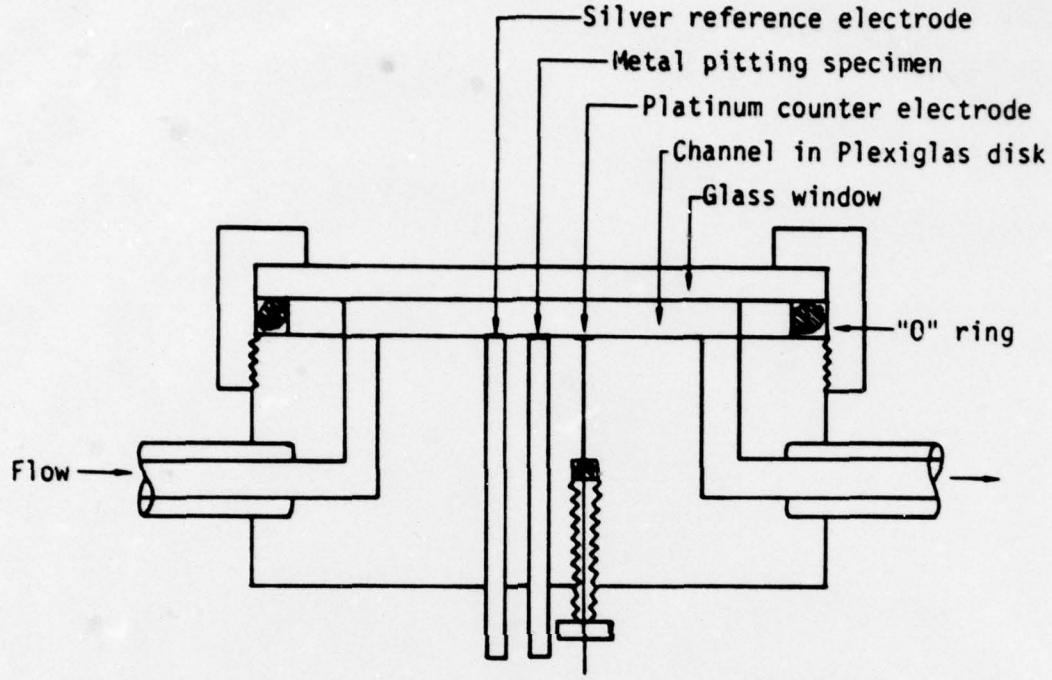

Fig. 1 Cutaway section of flow channel cell used to determine hydrodynamic effects on current density in small pits.

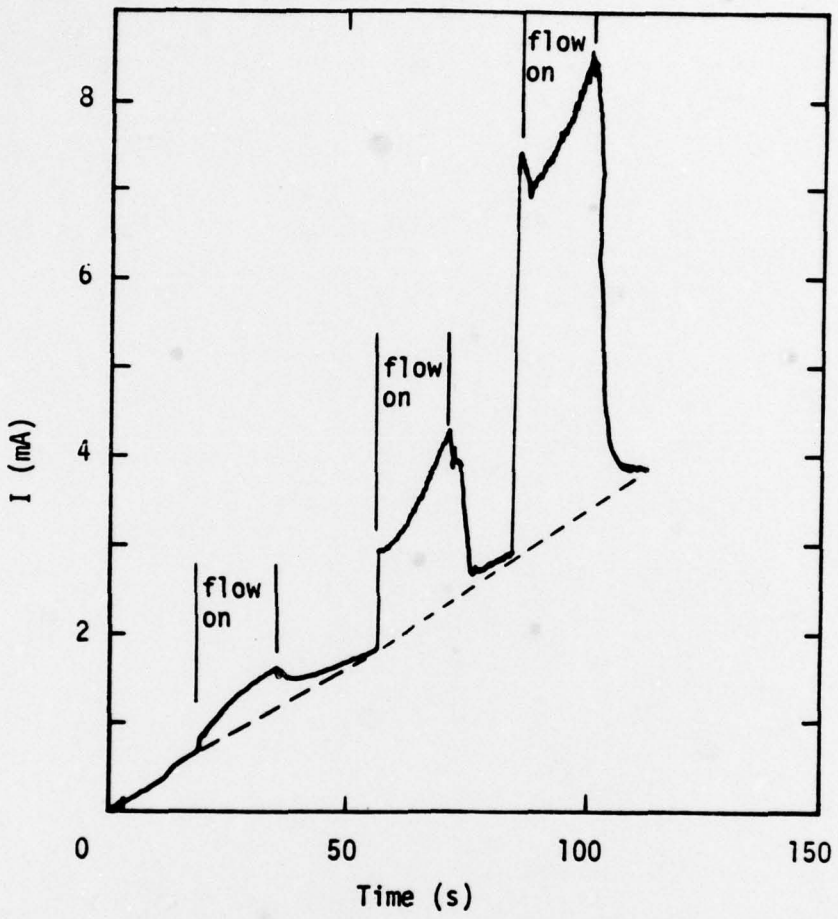

Fig. 2 Effect of flow (U = 155 cm/s) on pitting current for multiplicity of small pits in iron in 1 M Na_2SO_4 - 0.1 M NaCl solution at ϕ = 0.40 V_{SCE}.

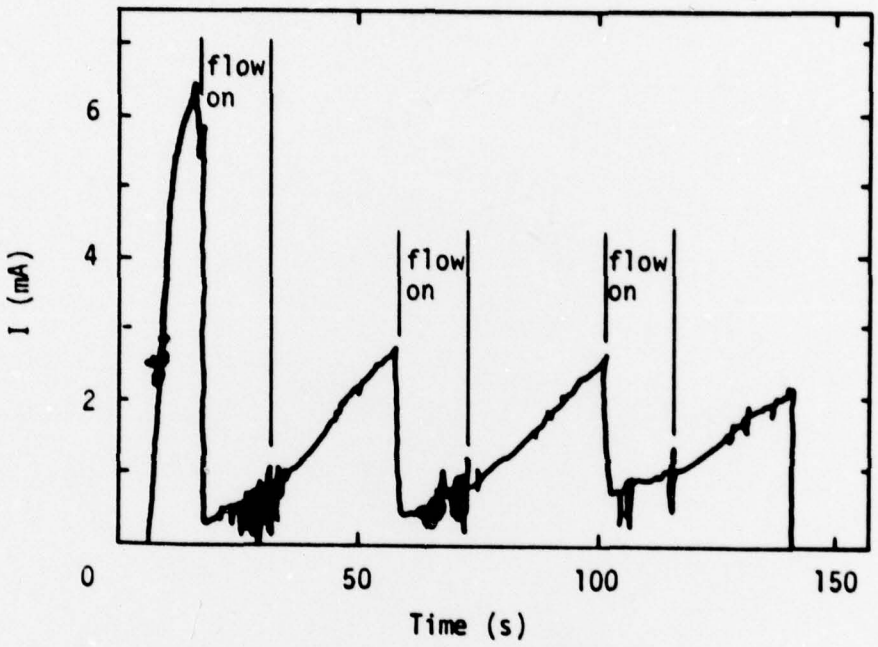

Fig. 3 Effect of flow (U = 155 cm/s) on pitting current for multiplicity of small pits in 304 stainless steel in 1 N NaCl at ϕ = 0.30 V_{SCE}.

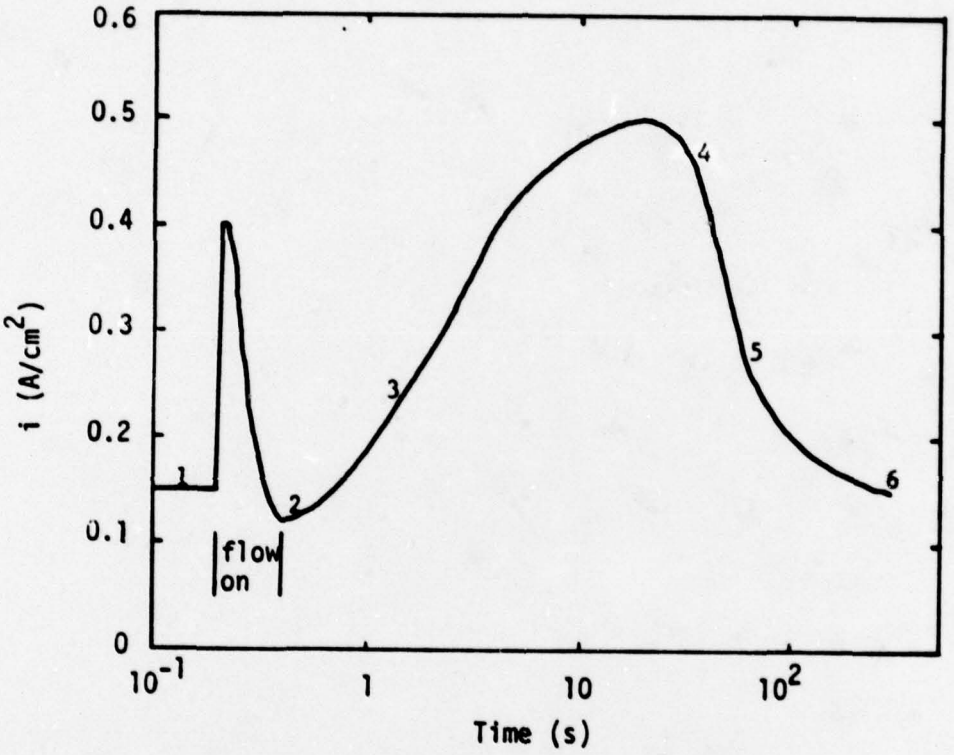

Fig. 4 Current transient for shielded electrode of 304 stainless steel, A = 0.050 cm^2, in 1 N NaCl, pH = 1, at ϕ = 0.80 V_{SCE} with electrolyte flow (U = 155 cm/s) and flow off.

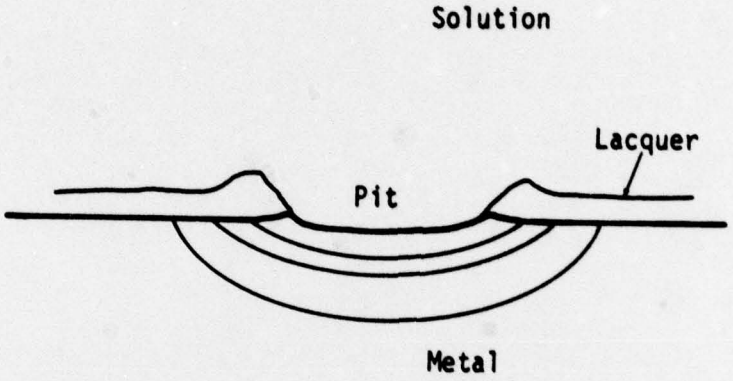

Fig. 5 Single artificial pit in hole in lacquer layer showing approximate corrosion profiles.

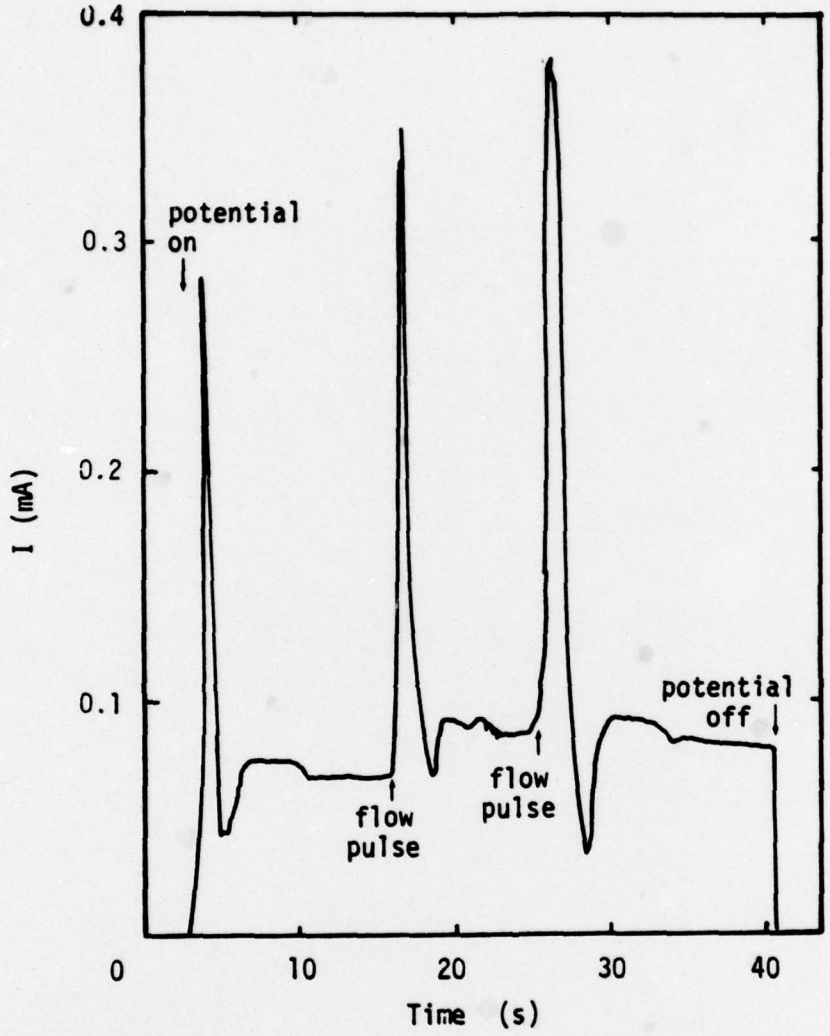

Fig. 6 Current transients to artificial pit in iron in 1 N NaCl, pH = 1, at ϕ = 0.20 V_{SCE} at turn on of potential and with electrolyte flow pulses.

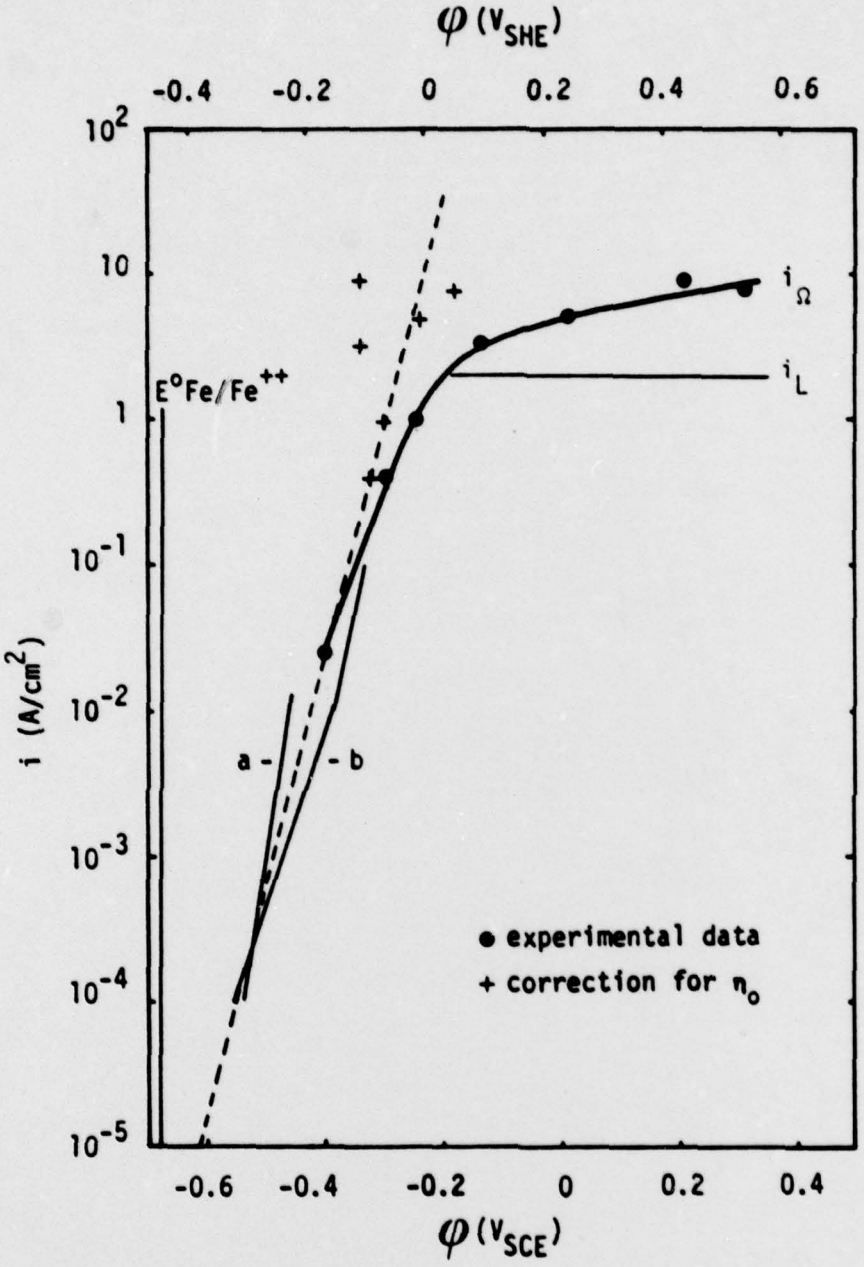

Fig. 7 Polarization curve for iron pits in 1 N NaCl at pH = 1 compared to literature data; a = 0.5 M $SO_4^=$, pH = 1 (Ref. 19); b = 4.5 M NaCl, pH = 1.2 (Ref. 20).

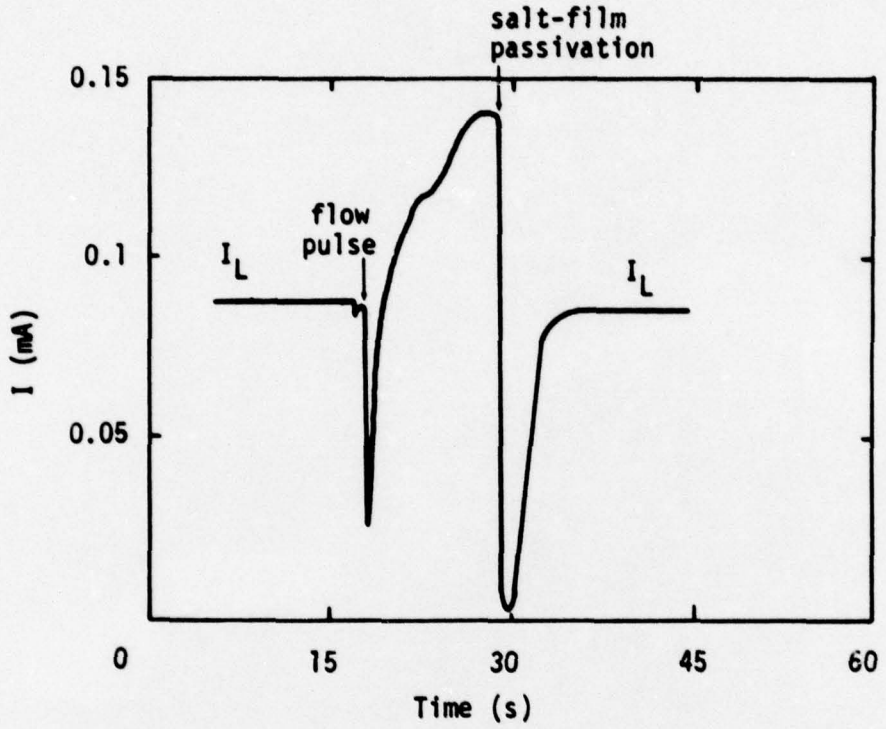

Fig. 8 Current transient to artificial pit in iron in 0.01 N NaCl at ϕ = 1.0 V_{SCE} with flow pulse of electrolyte.

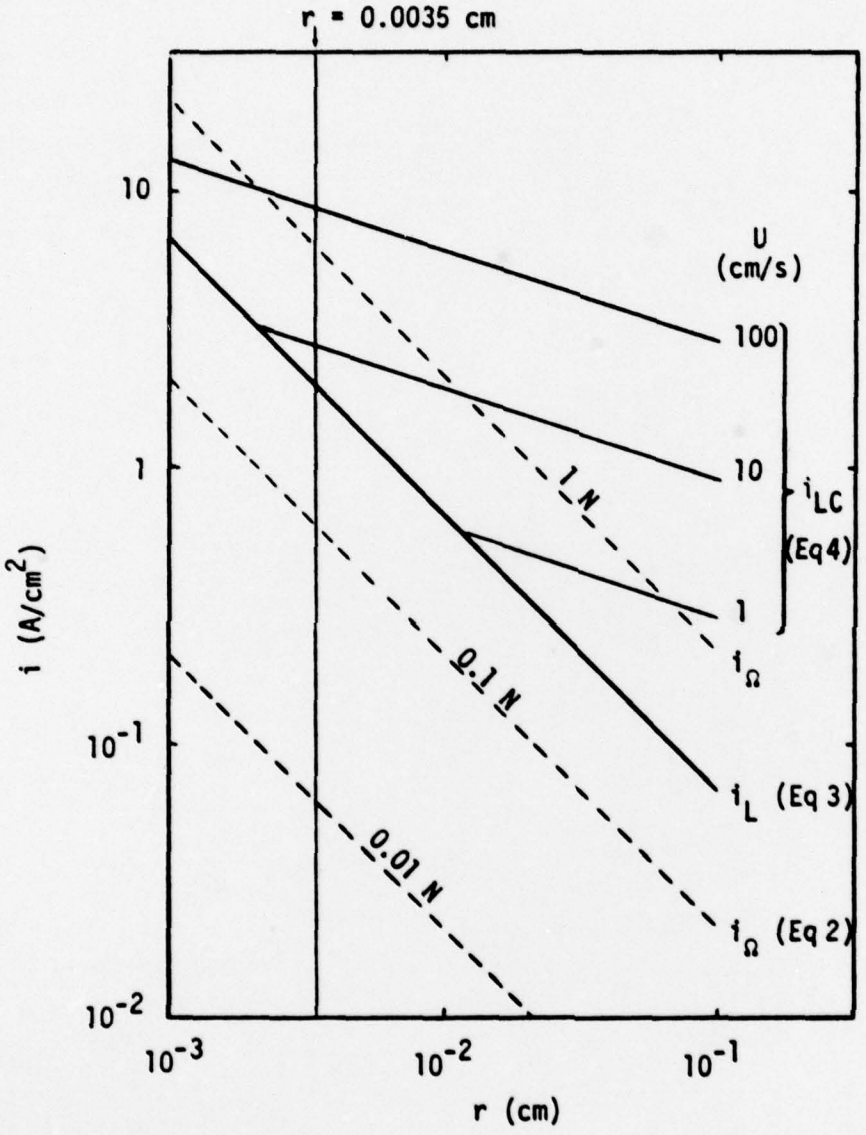

Fig. 9 Plots of equations 2, 3, and 4 (parameter values in Table 2).

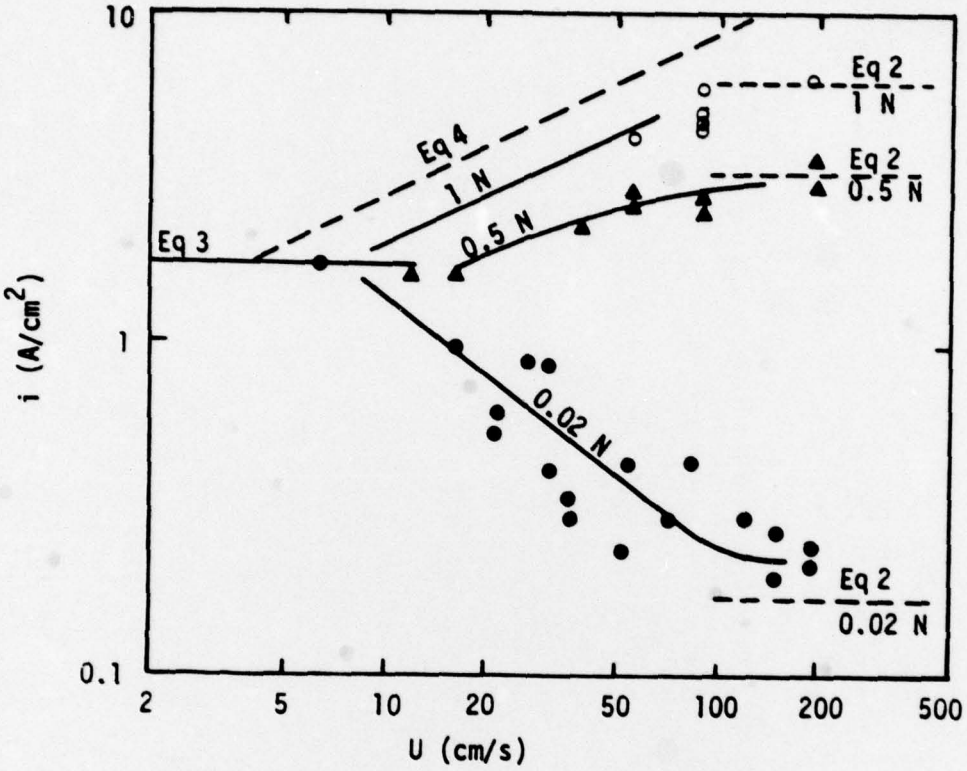

Fig. 10 Effect of flow velocity on current density in artificial pit, r = 0.0035 cm, in iron in NaCl solutions at ϕ = 0.30 V_{SCE} compared to predictions of equations 2, 3, and 4.

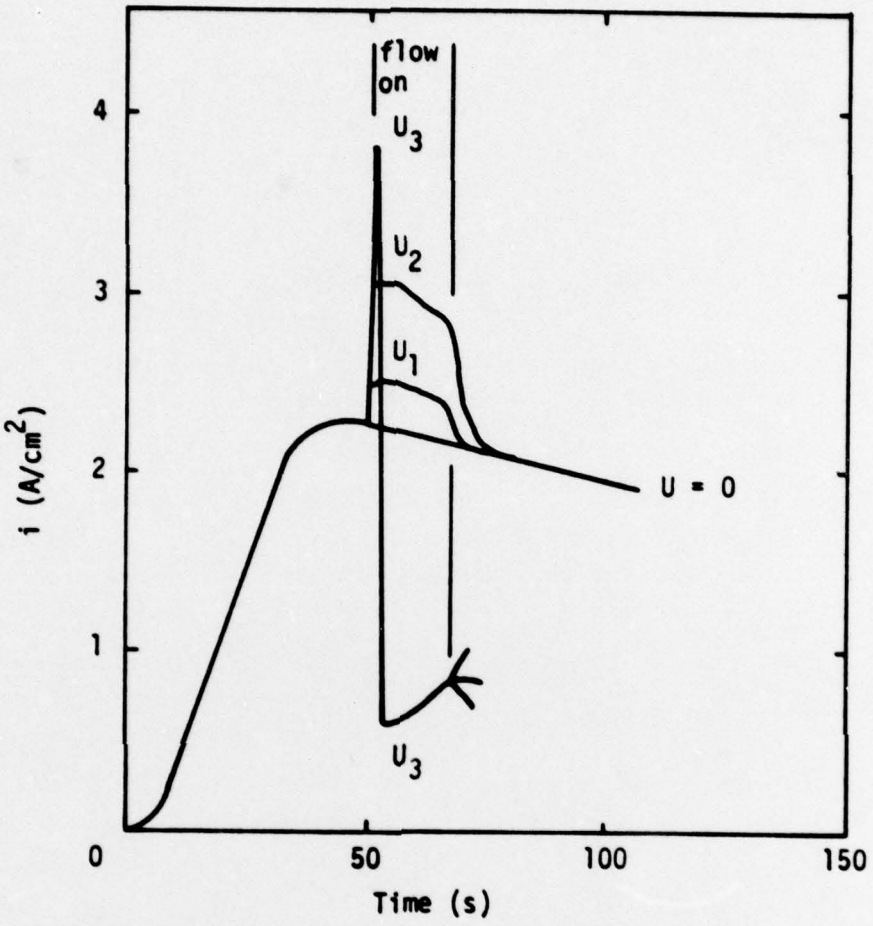

Fig. 11 Effect of flow velocity on current density in pit in 304 stainless steel, 1 N NaCl, 0.5 V_{SCE}, r = 6 x 10^{-3} cm. (A larger radius was used in order to more easily remove the hydroxide-salt layer.)

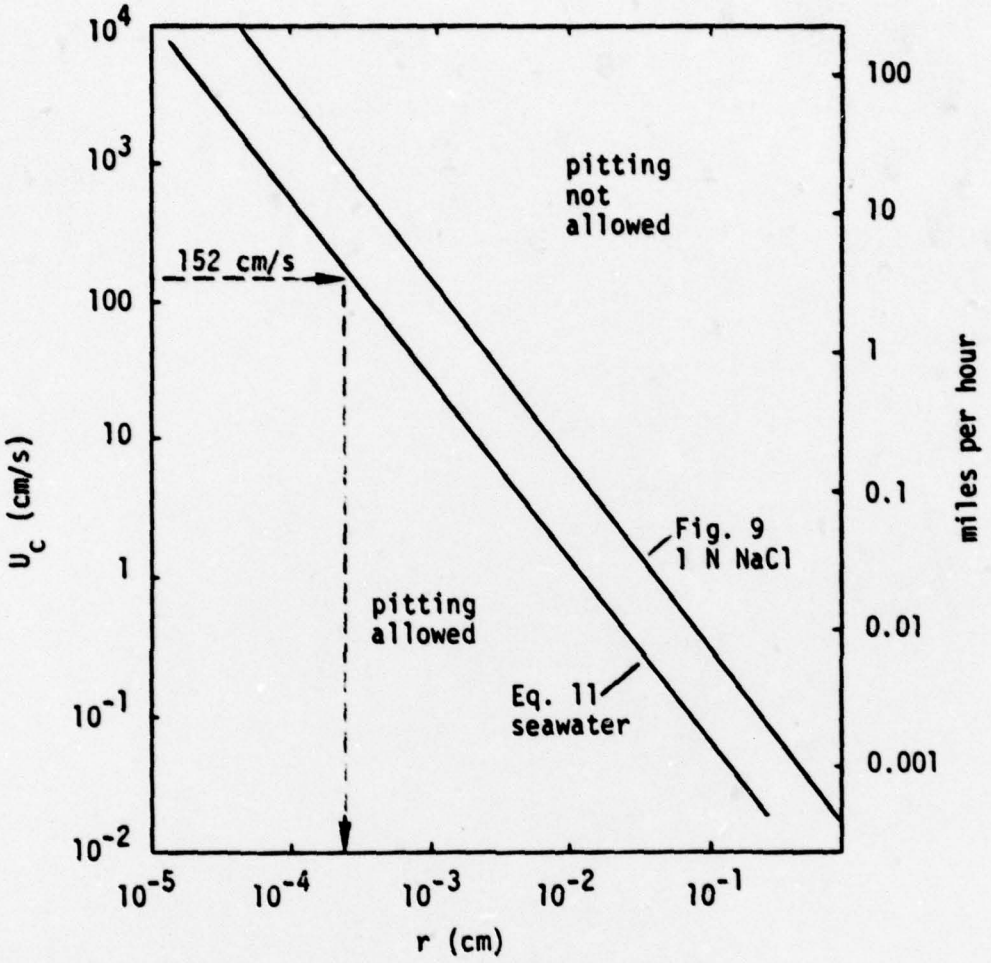

Fig. 12 Critical velocity for pitting of passivating metal as a function of pit radius.